The Astrophysical Journal, 617:1004–1016, 2004 December 20


# LUMINOUS COMPACT BLUE GALAXIES IN THE LOCAL UNIVERSE

Jessica K. Werk, Anna Jangren, and John J. Salzer
Astronomy Department, Wesleyan University, Middletown, CT 06459; jessica@astro.wesleyan.edu, anna@astro.wesleyan.edu, slaz@astro.wesleyan.edu
*Received 2004 June 30; accepted 2004 August 29*

## ABSTRACT

We use the KPNO International Spectroscopic Survey (KISS) for emission-line galaxies to identify and describe a sample of local analogs to the luminous compact blue galaxies (LCBGs) that are observed to be abundant at intermediate and high redshift. The sample is selected using criteria believed effective at isolating true examples of LCBGs: $SB_e(B\ \mathrm{band}) < 21.0$ mag arcsec$^{-2}$, $M_B < -18.5$ (for $H_0 = 75$ km s$^{-1}$ Mpc$^{-1}$), and $B - V < 0.6$. In addition, all LCBG candidates presented are selected to have star formation as their dominant form of activity. We examine the properties of our LCBGs and compare them with those of other KISS star-forming galaxies of the same absolute magnitude range. We find that the KISS LCBGs lie on the extreme end of a fairly continuous distribution of "normal" star-forming galaxies in the plane of surface brightness versus color. This result differs from the results of previous studies that show LCBGs at higher $z$ to be more separate from the "normal" (usually nonactive) galaxies with which they are compared. On average, LCBGs have a higher tendency to emit detectable flux in the radio continuum; have higher H$\alpha$ luminosities by a factor of 1.6, indicating strong star formation activity; and have slightly lower than expected metal abundances based on the luminosity-metallicity relation for KISS galaxies. We calculate the volume density of our low-$z$ ($z < 0.045$) sample to be $5.4 \times 10^{-4}\ h_{75}^3$ Mpc$^{-3}$, approximately 4 times lower than the volume density of the LCBGs at $0.4 < z < 0.7$ and $\sim$10 times lower than the volume density of the population at $0.7 < z < 1.0$.

*Subject headings:* galaxies: abundances — galaxies: active — galaxies: evolution — galaxies: starburst — galaxies: structure

## 1. INTRODUCTION

Common at intermediate and high redshifts, yet rare in the local universe, luminous compact blue galaxies (LCBGs) typically have luminosities equal to or greater than that of the Milky Way but are considerably smaller (Koo et al. 1994; Phillips et al. 1997; Guzmán et al. 1997; Östlin et al. 2001b; Mallén-Ornelas et al. 1999). As evidenced by such properties, they are among the most extreme galaxies known in the universe. Although these galaxies have been the subject of numerous comprehensive studies in the past decade, their evolution and nature, to a large extent, remain in dispute (Koo et al. 1995; Phillips et al. 1997; Hammer et al. 2001; Östlin et al. 2001a; Barton & van Zee 2001; Pisano et al. 2001; Guzmán et al. 2003). At the heart of the issue lies the difficulty of identifying nearby analogs that would allow a more complete exploration of the mechanisms responsible for their extreme properties at high redshifts, as well as their evolutionary paths.

Characterized by high surface brightnesses, small half-light radii, and vigorous star formation, LCBGs were initially identified as stellar objects from 4 m plate surveys for QSO candidates (Koo & Kron 1992; Koo et al. 1994; Guzmán et al. 1996, 1998). The formal definition of LCBGs is developed by A. Jangren et al. (2004, in preparation) by examining regions of six-dimensional parameter space (color, luminosity, asymmetry, concentration, size, and surface brightness) occupied by three classes of compact galaxies chosen to represent the population of luminous blue compact galaxies as a whole. The three classes are (1) compact narrow emission line galaxies (CNELGs; Koo et al. 1994, 1995; Guzmán et al. 1996, 1998); (2) a subset of galaxies very similar to CNELGs studied by Koo et al. (1995), Phillips et al. (1997), and Guzmán et al. (1997), called faint blue galaxies; and (3) higher redshift blue nucleated galaxies (Schade et al. 1995, 1996). While the classification of an LCBG relies on a galaxy's falling within three of five defined regions in the aforementioned parameter space, groups have recently adopted three cutoffs that roughly correspond to the criteria laid out by A. Jangren et al. (2004, in preparation): $B - V < 0.5$–$0.6$, $SB_e < 21$–$21.5$ mag arcsec$^{-2}$, and $M_B < -18.5$, with $H_0 = 70$ km s$^{-1}$ Mpc$^{-1}$ (Garland et al. 2004; Pisano et al. 2001). These selection criteria are further examined in subsequent sections.

With a volume density that drops off substantially from $z = 1$ to the present (previously estimated to be a change of roughly a factor of 10), LCBGs appear to be the most strongly evolving galaxy population (Lilly et al. 1996, 1998; Phillips et al. 1997; Guzmán et al. 1997; Mallén-Ornelas et al. 1999). Guzmán et al. (1997) estimate that they contribute nearly 40% of the fractional increase in the star formation rate (SFR) density between $z = 0$ and 1. Furthermore, luminous, compact star-forming galaxies (SFGs) appear to dominate high-redshift galaxy samples. Lowenthal et al. (1997) have suggested that the Lyman break galaxies at $z = 3$, because of their very compact cores and high surface brightnesses, may be the high-redshift counterparts of the intermediate-$z$ LCBGs. Smail et al. (1998), in a submillimeter galaxy survey, found a $z \sim 4$ galaxy population that may contribute a substantial fraction of the SFR density in the early universe, nearly half of which are very luminous and compact. Evidently, LCBGs play a prominent, if not paramount, role in the formation and evolution of galaxies in the young universe.

A drove of unanswered questions hovers around the subject of LCBGs, mainly for lack of a representative local sample. One of these questions involves the mechanism(s) responsible for the observed intense starbursts in LCBGs. In theory, these triggering mechanisms could be determined by examining the H$\alpha$ velocity fields and morphologies of local LCBG examples (Östlin et al. 2001a). This sort of study relies on the

assumption that one can select a sample of local LCBGs to have the same properties as the more distant LCBGs. (Östlin et al. 2001b) use a sample of six galaxies with $M_B$ between $-17.5$ and $-20$ selected from local blue compact galaxies (BCGs) that are bright in H$\alpha$ to infer certain kinematic properties of the higher $z$ LCBGs. They conclude that, in most cases, mergers or strong interactions trigger the intense starbursts of LCBGs. However, one should use caution in interpreting these results, given the size and properties of their sample. Indeed, a statistically complete sample of low-$z$ LCBGs would provide more clues as to the origin of their activity.

Another crucial topic in the study of LCBGs has been the question of what sort(s) of galaxy they become as they evolve. The determination of reliable mass estimates for the intermediate-$z$ LCBGs is key to establishing these evolutionary connections to present-day galaxies. However, accurate stellar mass estimates are difficult to determine, and measurements of emission-line widths used to indicate the virial mass may underrepresent the gravitational potential for the intermediate-redshift LCBGs (Guzmán 2001; Guzmán et al. 2003; Pisano et al. 2001). As a consequence of these difficulties, there is not good agreement for the mass estimates of LCBGs, and there is a corresponding uncertainty as to their proposed evolutionary path(s). Phillips et al. (1997), Barton & van Zee (2001), and Hammer et al. (2001) argue for an evolutionary scenario in which LCBGs represent the formation of the bulges of objects that eventually evolve into the massive spiral disks of today. Koo et al. (1995), and Guzmán et al. (1996, 1997, 1998) maintain that, while LCBGs represent a heterogeneous class of galaxies, the majority evolve into local low-mass dwarf elliptical galaxies.

A possible solution to the mass debate may lie in the H I line widths of local LCBGs. These line widths can be used to infer the total dynamical mass. Accordingly, Pisano et al. (2001) set out to measure the H I line widths of a nearby sample of galaxies they believe are representative of the more distant LCBGs. They infer the masses of the intermediate-$z$ galaxies from these local examples and find that LCBGs have a variety of dynamical masses and thus a variety of evolutionary paths. Yet, they recognize that their local sample may not be truly representative of the high-$z$ LCBG population. Of their 11 local galaxies, only three meet the criteria proposed by A. Jangren et al. (2004, in preparation). In a study of 20 local LCBG candidates selected to more nearly meet the criteria of A. Jangren et al. (2004, in preparation), Garland et al. (2004) found results similar to those of Pisano et al. (2001). Specifically, they show that while most LCBGs are nearly 10 times less massive than local galaxies of the same luminosity, some are just as massive. The implication is that LCBGs are a heterogeneous class of galaxy.

Clearly, defining reliable local samples of LCBGs is central to the process of understanding their nature and evolutionary paths. The Pisano et al. (2001) and Garland et al. (2004) samples are recent attempts to construct samples of nearby LCBGs. The latter study is based on a sample of LCBGs discovered by F. J. Castander et al. (2004, in preparation), who analyzed data from the Sloan Digital Sky Survey. Another recent study by Drinkwater et al. (1999) utilized the complete spectroscopic study of a 12 deg$^2$ area centered on the Fornax Cluster to identify a sample of 13 LCBGs with redshifts less than 0.21. In the current study, we take a slightly different approach.

Using the KPNO International Spectroscopic Survey (KISS; Salzer et al. 2000), we aim to identify and describe a statistically complete local sample of SFGs that best resemble those LCBGs observed in the more distant universe. Our low-$z$ sample will provide a basis for future work aimed at resolving the debates over the evolutionary histories and kinematics of LCBGs. Because of the limited resolution of the survey images, the classification scheme developed by A. Jangren et al. (2004, in preparation), which uses morphological parameters, cannot be employed. Instead, we apply selection criteria chosen to match those used by Guzmán (2003) and Garland et al. (2004) as a way to isolate the LCBGs from other KISS SFGs. While sharp boundaries in parameter space do not always effectively isolate one type of galaxy from another, LCBGs in the color–surface brightness plane occupy a well-defined region of parameter space (A. Jangren et al. 2004, in preparation). Therefore, we employ criteria in $B-V$ color, surface brightness, and luminosity to select a sample of local LCBG candidates. Still, none of the selection criteria we use can guarantee that the KISS LCBG candidates, like other putative local samples, contain bona fide LCBGs; they only ensure a similarity. Regardless, we believe that the sample that we define will provide an adequate starting point for future investigation. In § 2, we describe KISS, our measurements, and selection criteria. An analysis of the properties of our local LCBGs, along with the volume density calculation, appears in § 3. Section 4 contains a discussion of the implications our sample has for high-$z$ studies and potential future work on these galaxies beyond KISS. In § 5, we summarize our results. Throughout this paper, we adopt $H_0 = 75$ km s$^{-1}$ Mpc$^{-1}$.

## 2. DATA

### 2.1. *KPNO International Spectroscopic Survey*

KISS aims to find a quantifiably complete, well-defined sample of extragalactic emission-line sources (Salzer et al. 2000). Although this survey is not the first to look for galaxies that display unusual activity, it reaches substantially deeper than other wide-field objective-prism surveys, mainly because it *is* the first survey of this type to employ a large-format CCD as its detector. The survey data, composed of both objective-prism and direct images, were taken with the 0.61 m Burrell-Schmidt telescope located on Kitt Peak. The objective-prism images cover a spectral range of either 4800–5500 or 6400–7200 Å, and the direct images are observed through standard $B$ and $V$ filters. Our local sample of LCBGs is derived from the first three KISS survey strips: KISS red list 1, described in Salzer et al. (2001, hereafter KR1); KISS blue list 1, described in Salzer et al. (2002, hereafter KB1); and KISS red list 2, described in Gronwall et al. (2004b, hereafter KR2). KR1and KR2 use the H$\alpha$ line for selection, whereas KB1 detects objects by their [O III] emission line. The KR1 portion of KISS finds 1128 emission-line galaxy (ELG) candidates in a survey area of 62.2 deg$^{-2}$ (or 18.1 KISS ELGs deg$^{-2}$), the KB1 portion of KISS finds 223 ELG candidates in 116.6 deg$^2$ (or 1.91 KISS ELGs deg$^2$), and the KR2 portion of KISS finds 1029 ELG candidates in 65.8 deg$^2$ (or 15.6 KISS ELGs deg$^{-2}$). KR1 and KB1 overlap with part of the Century Survey (CS; Geller et al. 1997; Wegner et al. 2001), while KR2 runs through the center of the Bootes void.

The KISS data are run through several steps of processing using a series of IRAF[1] scripts: object detection and inventory, photometry and object classification, astrometry, spectral image coordinate mapping and background subtraction, spectral extraction and overlap correction, emission-line detection, and spectral parameter measurement. Measurements of the

[1] IRAF is distributed by the National Optical Astronomy Observatory, which is operated by the Association of Universities for Research in Astronomy, Inc., under cooperative agreement with the National Science Foundation.

extracted objective-prism spectra yield estimates of the redshifts, line fluxes, and equivalent widths of the ELGs. For a complete description of the data processing, see Salzer et al. (2000). It should be noted that many objects are unresolved in the direct images (which have a resolution of $\sim 4''$); it is not necessary for an object to be classified morphologically as a galaxy to be included in the ELG list. The only criterion for inclusion is the presence of an emission line in the objective-prism spectrum. In other words, there is no bias against compact, stellar-appearing objects in KISS.

Although the survey data themselves provide considerable information about the sources, obtaining follow-up spectra is an important part of the KISS project. These spectra provide higher quality redshifts, confirm ELG candidates' status as actual ELGs, and provide the means by which to identify the type of activity powering the ELG. In most cases, emission lines such as H$\alpha$, H$\beta$, [O III] $\lambda\lambda$4959, 5007, and [N II] $\lambda\lambda$6548, 6583 are present in the follow-up spectra. With the higher accuracy line strengths of these spectra, one can distinguish between SFGs, Seyfert 1 galaxies, Seyfert 2 galaxies, LINERs, and QSOs. Furthermore, determination of the metallicity (Melbourne & Salzer 2002; Melbourne et al. 2004; Lee et al. 2004; Salzer et al. 2004) and the SFR is possible with accurate line strength measurements. Follow-up spectra have been obtained for 83% of the KR1 ELGs, 100% of the KB1 ELGs, and 30% of the newer KR2 ELGs at various telescopes, including the Hobby-Eberly telescope (Gronwall et al. 2004a), the Michigan-Dartmouth-MIT 2.4 m telescope (Wegner et al. 2003), the Wisconsin-Indiana-Yale-NOAO (WIYN) 3.5 m telescope, the 2.1 m telescope on Kitt Peak, the Apache Point Observatory 3.5 m telescope, and the Shane 3.0 m telescope at Lick Observatory (Melbourne et al. 2004).

### 2.2. *Surface Brightness and Half-Light Radius Measurements*

LCBGs typically are identified by their small half-light radii ($r_{\rm hl}$) and/or their high surface brightnesses (SB$_e$). Therefore, measuring these quantities in the KISS data was an essential first step in our effort to isolate a sample of nearby LCBGs. We wrote an IRAF procedure called KCOMPACT to find $r_{\rm hl}$ for every object in the KISS survey images. The procedure performs a curve-of-growth analysis using circular apertures to determine $r_{\rm hl}$. The formal uncertainty in $r_{\rm hl}$ is estimated by comparing the separate measurements of ELGs present in two survey fields (the overlap in adjacent KISS fields is approximately $3'$–$5'$). Based on 14 objects, we determine the uncertainty in $r_{\rm hl}$ to be $0\farcs21$. Combining our estimates of $r_{\rm hl}$ with the total apparent magnitude measured during the KISS data processing (see § 2.1) allows us to compute SB$_e$ using the following formula:

$$\mathrm{SB}_e = m_B + 0.753 + 2.5 \log \pi r_{\rm hl}^2. \quad (1)$$

As the formal errors in the KISS apparent magnitudes are always below 0.1 mag, we can find the upper limit on the uncertainty of SB$_e$ due to the errors in $m_B$ and $r_{\rm hl}$. We find $\sigma_{\mathrm{SB}_e} < 0.14$ mag arcsec$^{-2}$.

The reliability of $r_{\rm hl}$ and SB$_e$ is inextricably linked to the resolution of the image on which they are measured. Both the image scale and the effective seeing significantly affect the accuracy of these quantities. Resolution limits restrict the precision with which these quantities can be determined in the more distant portion of KISS. Since *all* objects in each survey image are analyzed by KCOMPACT, we use the locus of the $r_{\rm hl}$ values for objects previously identified as stars to define a rough resolution limit for each image. Marked interactively, the resolution limit does not represent the mean FWHM of the stellar distribution but rather is selected to encompass the entire locus of stellar objects. As we discuss in the following paragraph, variable image quality across our survey images causes this limit to underestimate the true image quality for a modest fraction of our ELG candidates. For KB1 and KR1, the mean resolution limit (i.e., the lower limit on $r_{\rm hl}$) of the images is $2\farcs50$ compared with an image scale of $2\farcs03$ pixel$^{-1}$; for KR2, this mean resolution limit of the images is $2\farcs13$ compared with an image scale of $1\farcs43$ pixel$^{-1}$. Therefore, objects with $r_{\rm hl}$ under $2\farcs5$ are almost always unresolved (or, at best, marginally resolved) in the KISS survey direct images. Moreover, as the distance to an object increases, so does the physical diameter that corresponds to this resolution limit; that is to say, at greater distances, galaxies with progressively larger diameters dominate any resolved sample. Figure 1 shows this effect, plotting diameter in kiloparsecs versus distance in megaparsecs, where the diagonal lines represent the nearly constant resolution limits (converted to kiloparsecs) below which an object is unresolved. Everything but galaxies with large diameters are unresolved at the redshift limit of the survey. Ultimately, this bias leads us to adopt a distance-limited sample of KISS LCBGs (see § 2.3).

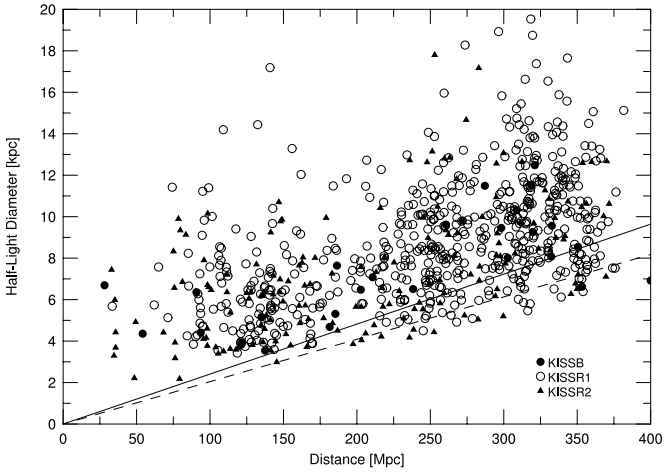


FIG. 1.—Half-light diameter in kiloparsecs vs. the distance in megaparsecs for a subset of KISS SFGs from each survey strip. The dashed line represents the diameter (in kiloparsecs) necessary for a KR2 object to be resolved at a given distance (based on the rough-resolution limit discussed in § 2.2). The solid line represents the diameter (in kiloparsecs) necessary for KB1 and KR1 objects to be resolved at a given distance. Below these lines, galaxies from their respective survey lists are unresolved.

The rough resolution limit discussed in the previous paragraph suffices to determine an appropriate distance cut (see below) but fails to account for the rather extreme image quality variability of the KISS direct images. The delivered image quality of the Burrell-Schmidt 0.61 m telescope at the time KISS was carried out could vary between $2\farcs5$ and $6\farcs5$ over a single survey field. Hence, rather than use a single value to describe the image quality on a given survey image, it is necessary to estimate the local value for the image quality in the vicinity of each KISS ELG. An IRAF script was written for this purpose. By locating the 10 stars closest to each ELG and measuring the FWHM of their profiles, this script accounts for the variable image quality of the KISS direct images. The local FWHM (average seeing) for each KISS ELG is the mean of the FWHM from the 10 stellar profiles. As our study relies on accurate measurements of $r_{\rm hl}$ and SB$_e$, we were forced to

exclude those objects for which the local image quality was severely degraded. A ratio between the mean local FWHM and the half-light diameter acted as our main diagnostic: if the ratio was above 1, we could not trust the measurement of $r_{hl}$, and therefore we excluded the galaxy. In addition, all objects with a local stellar FWHM above 5″ and a diagnostic ratio above 0.7 were also excluded. In total, 96 galaxies were cut out of the survey area, decreasing the area over which we could search for LCBGs by only ∼4%. With these exclusions, we feel confident in the completeness of our sample; that is, in the remaining portions of KISS, we should not miss any apparently small, potential LCBG candidate simply because it is unresolved. Of course, the galaxies remaining in our sample of KISS ELGs are not all well resolved, but, as we describe, we can account for the inaccuracies in their measurements.

In essence, our measurements of marginally resolved galaxies act as upper limits on $r_{hl}$ and lower limits on $SB_e$. We explore the nature of our unresolved and marginally resolved LCBG candidates using higher resolution images from the WIYN 0.9 m telescope on Kitt Peak. In 2003 May and 2004 March, we observed 11 KISS ELGs from KR1 and 12 KISS ELGs from KR2 under nonphotometric conditions with the S2KB CCD, for which the image scale is 0.″6 pixel$^{-1}$. The preexisting KISS direct images for the galaxies, which were taken under good conditions, provided the photometric calibration for our 0.9 m images. Despite the different image scales of KR1 and KR2, we treat them the same in the following analysis because of the variable image quality described above.

For the KISS compact, star-forming ELGs in each survey strip, we remeasured the half-light radii on the 0.9 m images using the same curve-of-growth routine described above and compared them with the values of $r_{hl}$ obtained in the same way for the KISS images. The KISS $r_{hl}$ is plotted against the ratio of the 0.9 m $r_{hl}$ to the KISS $r_{hl}$ in Figure 2*a* to show the results of these remeasurements. The triangles represent the ELGs from KR2, while the circles represent the ELGs from KR1. The relationship is equivalent for both strips: those objects with larger $r_{hl}$ have a ratio close to unity, while those objects with $r_{hl}$ near our resolution limits have ratios that deviate more considerably from unity.

We sought to quantify the correlation seen in Figure 2*a* to develop a correction of $r_{hl}$ for all unresolved and marginally resolved ELGs in the KISS database. Analyzing our sets of measurements for the 0.9 m images and the KISS images, we can predict the way in which the difference between a galaxy's 0.9 m $r_{hl}$ and its KISS $r_{hl}$ ($\Delta r_{hl}$) increases as its $r_{hl}$ decreases below the resolution limits of KISS. Instead of reobserving all unresolved and marginally resolved KISS ELGs to achieve more accurate measurements of their $r_{hl}$, we can infer the values we would obtain. Two of the 11 KR1 and 2 of the 12 KR2 ELGs observed with the WIYN telescope had $r_{hl}$ values greater than 6.″0 and were thus very well resolved in the KISS direct images. Figure 2*a* reassures us that our measurements of $r_{hl}$ on the 0.9 m images are very close to our measurements on the KISS images for these four well-resolved galaxies. These four galaxies were excluded from the determination of our correction. On closer examination of the 0.9 m images, one galaxy in KR1 was observed to have a merging partner, making any measurement of its $r_{hl}$ suspect. An additional two galaxies from each survey strip were excluded as well because they suffered from noticeably poorer image quality in the KISS direct images, skewing the relationships shown in the following plots. Figure 2*b* shows $\Delta r_{hl}$ versus the KISS $r_{hl}$ for the 14 remaining galaxies. In this figure, we note the same effect as in Figure 2*a*:

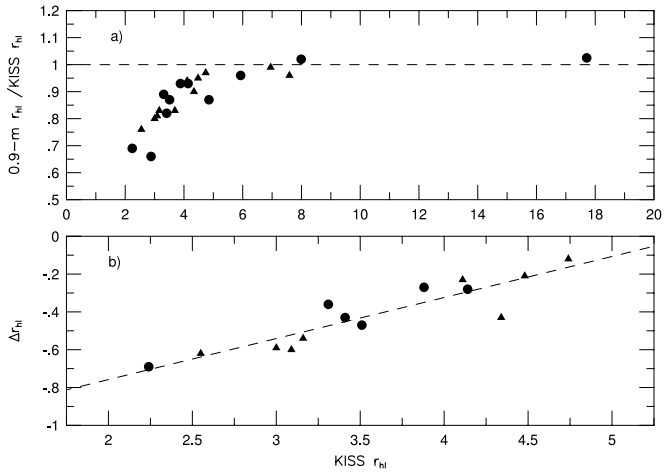


FIG. 2.—(*a*) Ratio of the $r_{hl}$ remeasured on the 0.9 m images (0.9 m $r_{hl}$) to the $r_{hl}$ measured on the KISS direct images (KISS $r_{hl}$) vs. the KISS $r_{hl}$. The circles represent ELGs from KR1, and the triangles represent ELGs from KR2. At an $r_{hl}$ of approximately 5″, the ratio of the two quantities is very close to 1. (*b*) Observed relation between $\Delta r_{hl}$(0.9 m $r_{hl}$ − KISS $r_{hl}$) and the KISS $r_{hl}$. Symbols are the same as in (*a*).The linear least-squares fit (*dashed line*) was used to apply a correction for the $r_{hl}$ of all KISS star-forming ELGs with $r_{hl}$ below 5″.

apparently smaller galaxies have greater $\Delta r_{hl}$. We based the final correction for $r_{hl}$ on the linear least-squares fit of the 14 data points plotted in Figure 2*b*. The fit is shown by the dashed line. The equation for this line is $\Delta r_{hl} = 0.22(\text{KISS } r_{hl}) - 1.19$, where $\Delta r_{hl}$ is in arcseconds and the scatter about the fit is 0.″11.

We also compared the apparent *B*-band magnitudes ($m_B$) measured on the 0.9 m and KISS images. Since our photometric calibration of the 0.9 m images used the original KISS calibration, our 0.9 m values for $m_B$ agree well with the KISS values for $m_B$. This remeasurement of $m_B$, combined with the correction for $r_{hl}$ described above, is relevant for probing the effects of low resolution on the measurement of $SB_e$ (see eq. [1]). Figure 3 plots the observed relation between $\Delta SB_e$ (0.9 m $SB_e$ − KISS $SB_e$) and $\Delta r_{hl}$. Since the KISS and 0.9 m apparent magnitudes show good agreement, the difference in the measured values of $SB_e$ must be solely due to the change in $r_{hl}$ between the KISS and 0.9 m images. Therefore, we can compute the correction for the effective surface brightness, $\Delta SB_e$, such that it depends on only $\Delta r_{hl}$:

$$\Delta SB_e = -2.5 \log \frac{r_{hl}^2}{(r_{hl} + \Delta r_{hl})^2}. \quad (2)$$

Figure 3 plots the observed values of $\Delta SB_e$ and $\Delta r_{hl}$ for the 14 KISS ELGs, along with a curve illustrating the analytical correction given by equation (2). The observed values of $\Delta r_{hl}$ and $\Delta SB_e$ are shown by the triangles (KR2) and the circles (KR1). In the equation, $\Delta r_{hl}$ corresponds to the linear least-squares fit shown in Figure 2*b* for the $r_{hl}$ correction. Figure 3 shows that the actual measurements of $\Delta r_{hl}$ and $\Delta SB_e$ follow the correction defined by equation (2) very well.

We apply these corrections for $r_{hl}$ and $SB_e$ to all nonexcluded (see above) KISS SFGs with an $r_{hl}$ value less than 5″. Among all KR1 star-forming ELGs with $r_{hl}$ under 5″ (i.e., those affected by the correction), the mean change in $r_{hl}$ is −0.″50, the mean change in diameter is −4.91 kpc, and the mean change in $SB_e$ is −0.44 mag arcsec$^{-2}$. Among all KR2

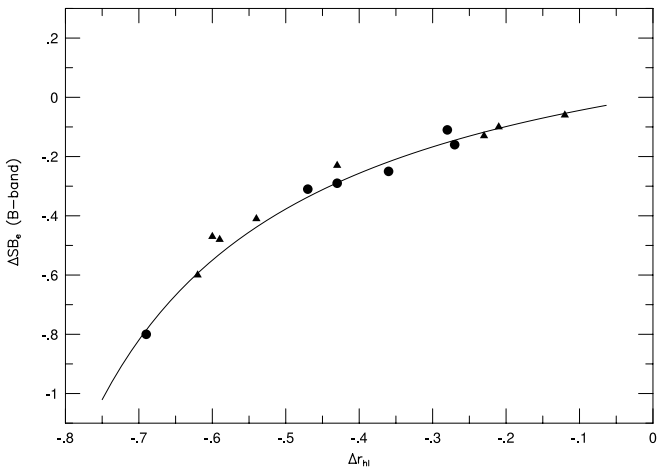


FIG. 3.—Observed relation between $\Delta SB_e$ (0.9 m $SB_e$ − KISS $SB_e$) and $\Delta r_{hl}$, shown by the circles and triangles, plotted with the analytical correction curve given by the equation $\Delta SB_e = -2.5 \log (r_{hl}^2/(r_{hl} + \Delta r_{hl})^2)$. The circles represent KR1 galaxies, while the triangles represent KR2 galaxies. The quantity $\Delta r_{hl}$ is based on the correction for $r_{hl}$, given by the linear least-squares fit shown in Fig. 2.

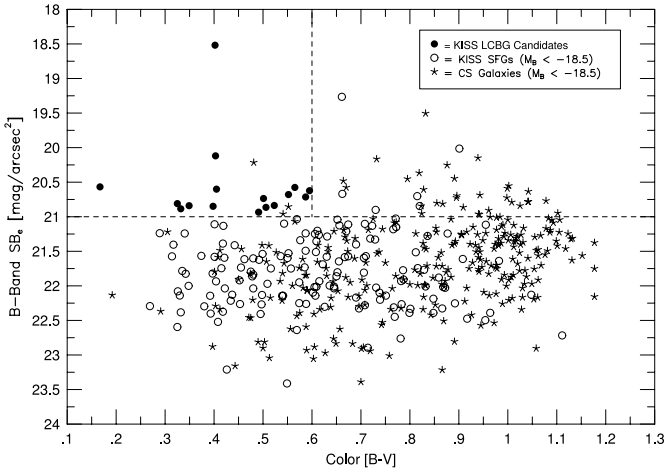


FIG. 4.—Effective $B$-band surface brightness plotted against $B - V$ color for the KISS SFGs and CS galaxies within 185 Mpc of the Milky Way, showing the selection cutoffs for the KISS LCBG sample (*dashed lines*), galaxies from the CS (*stars*), and the KISS SFGs (*open circles*). We see that 16 ELGs compose the distance-limited LCBG sample (*filled circles*).

star-forming ELGs with $r_{hl}$ under 5″, the mean change in $r_{hl}$ is −0.″56, the mean change in diameter is −5.31 kpc, and the mean change in $SB_e$ is −0.57 mag arcsec$^{-2}$.

### 2.3. *Sample Selection*

The ability of our local LCBG candidates to provide meaningful mass and SFR comparisons with the higher $z$ LCBGs requires that these galaxies be genuine LCBGs. Typical methods of identifying nearby LCBG analogs usually employ cutoffs in surface brightness, luminosity, and color and cannot guarantee that the galaxies are true examples of LCBGs. Indeed, we can pick out only those galaxies that are *likely* to be LCBGs. Considering the nature of KISS, we believe that we are identifying those ELGs that possess the same properties as the LCBGs at intermediate and high redshifts and thus those galaxies that are most likely to be true LCBGs. Hence, we call our galaxies "LCBG candidates."

In an attempt to match our KISS LCBG sample with the higher redshift samples, we endeavor to employ the same cutoffs as those used in earlier work. The sample is based on criteria proposed by Guzmán (2003), who uses cutoffs in surface brightness, rest-frame color, and absolute magnitude for the selection of LCBGs. All criteria are limited by the angular resolution of the KISS direct images. Certainly, LCBGs are *not* active galactic nuclei and are most often characterized by vigorous star formation. Therefore, the sample was selected from a subsample of KISS galaxies known from follow-up spectra to have star formation as their primary activity. All values given for $B - V$ color and all magnitudes used in the KISS sample selection are corrected for Galactic absorption using the values of Schlegel et al. (1998). In addition, to select this sample, we used the corrected values of $SB_e$ determined from the analysis outlined in § 2.2.

A total of 17 KISS SFGs meet the selection criteria proposed by R. Guzmán: $SB_e(B \text{ band}) < 21.0$ mag arcsec$^{-2}$, $M_B < -18.5$, and $B - V < 0.6$ with $H_0 = 70$ km s$^{-1}$ Mpc$^{-1}$. We use this absolute magnitude limit for the selection of KISS LCBGs despite our use of $H_0 = 75$ km s$^{-1}$ Mpc$^{-1}$ by KISS. Since this absolute magnitude cut corresponds to $M_B < -18.35$ with $H_0 = 75$ km s$^{-1}$ Mpc$^{-1}$, we apply a slightly more stringent cut for absolute magnitude by 0.15 mag when we use $M_B < -18.5$ as one of our selection criteria.

This sample of LCBGs is partially determined by the resolution selection effects described in § 2.2 and shown in Figure 1. These effects dictate that the majority of identified LCBG candidates are located at distances far closer than the KISS redshift limit of $z = 0.095$. When we consider that the median half-light diameter of the 17 LCBGs is 4.21 kpc, Figure 1 indicates that the likelihood of finding an LCBG beyond ∼200 Mpc is low. A further implication of this effect is that any comparison of the KISS LCBG sample with other KISS SFGs would be skewed. KISS SFGs detected at greater distances would be, on average, considerably larger in diameter and more luminous. To account for these effects and to improve the completeness of our LCBG sample, we impose on it a distance limit of 185 Mpc ($z \sim 0.045$). Of the 17 KISS LCBGs, 16 lie within this boundary, and according to the resolution thresholds marked on Figure 1, any galaxy within 185 Mpc of the Milky Way with a diameter equal to or greater than ∼4 kpc would be resolved in the KISS images.

Figure 4 shows the KISS ELGs that lie within 185 Mpc of the Milky Way and have $M_B < -18.5$. The 16 KISS ELGs that remain in the sample after the application of the distance cutoff are marked as filled circles in the plot, and the dashed lines indicate two of the selection criteria. The stars in the plot represent a subset of "normal" galaxies from the CS carried out by Wegner et al. (2001) that lie within the distance limit and have $M_B < -18.5$. The CS is a traditional magnitude-limited survey of "normal" field galaxies that are used here to represent the general galactic population. The open circles represent a comparison sample of KISS star-forming ELGs that have $M_B < -18.5$ and lie within 185 Mpc of the Milky Way. Henceforth, when we refer to our samples of LCBG candidates and comparison samples, we refer to the "*distance-limited* samples." It should be noted that all KISS ELGs selected as LCBG candidates have been identified from follow-up spectra as having star formation as their primary activity.

On the plot of $SB_e$ versus color in Figure 4, two features stand out. While the KISS LCBG candidates were selected to have surface brightnesses higher than the typical SFG, even the highest surface brightness LCBG candidates do not appear

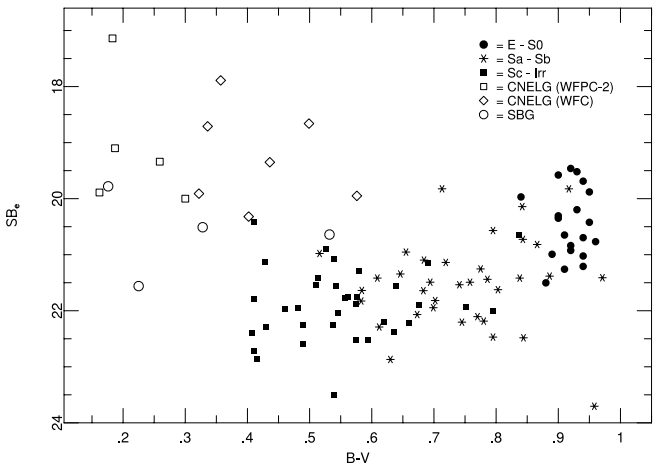


FIG. 5.—Rest-frame effective $B$-band surface brightness, $SB_e$, vs. rest-frame color, $B - V$. In this plot from A. Jangren et al. (2004, in preparation), the CNELGs and small blue galaxies (SBGs), also called faint blue galaxies, come from Koo et al. (1994, 1995), while the "normal" Hubble-type galaxies come from a catalog assembled by Frei et al. (1996). Here the LCBGs (CNELGS and SBGs) are clearly separated from the "normal" galaxies. We saw a similar effect in Fig. 4 for the LCBGs vs. the CS galaxies. In contrast, we saw in the same figure that the LCBGs seem to be on the high surface brightness end of a continuous distribution of regular SFGs.

to be clearly separated from the distribution of KISS SFGs. Instead, the SFGs form a more nearly continuous distribution in color and $SB_e$, as one might expect. At intermediate redshifts, A. Jangren et al. (2004, in preparation) find that in the parameter space of $SB_e$ and $B - V$ color, LCBGs separate themselves more cleanly than in any other parameter space from ordinary irregular, elliptical, and spiral galaxies. A plot from A. Jangren et al. (2004, in preparation), illustrating this separation, is shown in Figure 5. When we compare LCBGs with the other KISS SFGs, we do not see this effect. In the $z < 0.045$ local universe, the bluest, highest surface brightness star-forming ELGs do not appear to be separate from a distribution of otherwise regular SFGs but rather represent the most extreme galaxies in this class of star-forming ELGs. However, the KISS LCBG candidates are more clearly separate from the CS galaxies. Interesting to note is that, while only three of the CS galaxies meet the selection criteria for an LCBG, 29 CS galaxies redder than the color cut meet both the surface brightness and absolute magnitude cut. We believe these 29 galaxies to be local normal elliptical galaxies. Only six KISS ELGs fall in this region of the diagram (i.e., compact but red).

The properties of the 16 ELGs selected as local LCBG candidates are listed in Table 1. Columns (1) and (2) give the survey identification numbers for each galaxy (KISSR and KISSB numbers). The apparent $B$-band magnitude is listed in column (3), the $B$-$V$ color in column (4), the half-light diameter in kiloparsecs in column (5), the $B$-band effective surface brightness ($SB_e$) in column (6), the distance to the galaxy (in megaparsecs) in column (7), the absolute $B$-band magnitude in column (8), the logarithm of the H$\alpha$ luminosity in column (9), and the logarithm of the 1.4 GHz radio power from Van Duyne et al. (2004) in column (10). Those galaxies without a listed radio power were not detected as radio emitters in the Van Duyne et al. study.

Images of the 16 LCBG candidates made from the KISS direct images appear in Figure 6. Although the resolution of KISS is too low for measuring parameters such as asymmetry and concentration, we can see some of the morphological characteristics of our LCBG candidates on these images. At least three of the LCBG candidates, KISSR 147, 1274, and 1870, appear to have disturbed morphologies, evidence for recent interactions and/or mergers. However, the majority of the 16 LCBG candidates appear to be small, compact, and quite symmetric, suggesting that interactions are not the main driver of the observed star formation activity in most cases.

## 3. PROPERTIES OF THE LOCAL LCBG CANDIDATES

### 3.1. *Global Characteristics*

The KISS project obtains photometrically calibrated $B$ and $V$ direct images, along with the objective-prism spectra, that provide accurate measurements of each galaxy's H$\alpha$ flux. In addition, all our LCBG candidates have been observed as part of our follow-up spectroscopy program (e.g., Wegner et al. 2003; Gronwall et al. 2004a). Hence, there is a large amount of information readily available for all KISS ELGs that allows

TABLE 1
A KISS SAMPLE OF LCBG CANDIDATES

| KISSR Number (1) | KISSB Number (2) | $m_B$ (3) | $B - V$ (4) | Diameter (kpc) (5) | $SB_e$ (mag arcsec$^{-2}$) (6) | Distance (Mpc) (7) | $M_B$ (8) | $\log L_{H\alpha}$ (ergs s$^{-1}$) (9) | $\log P_{1.4\,GHz}$ (W Hz$^{-1}$) (10) |
|---|---|---|---|---|---|---|---|---|---|
| 113 | ... | 15.36 | 0.40 | 1.53 | 18.52 | 93 | −19.48 | 40.46 | ... |
| 147 | ... | 12.44 | 0.55 | 6.53 | 20.68 | 33 | −20.18 | 39.59 | 22.19 |
| 218 | ... | 15.34 | 0.49 | 4.21 | 20.93 | 84 | −19.29 | 41.20 | 21.60 |
| 242 | 128 | 16.66 | 0.35 | 4.02 | 20.84 | 153 | −19.26 | 41.72 | 21.62 |
| ... | 169 | 16.56 | 0.51 | 3.39 | 20.86 | 122 | −18.87 | 41.14 | ... |
| 707 | 189 | 14.99 | 0.40 | 5.42 | 20.85 | 94 | −19.87 | 41.64 | 21.41 |
| 1094 | 218 | 15.24 | 0.41 | 6.08 | 20.60 | 134 | −20.40 | 41.91 | 21.86 |
| 1271 | ... | 17.33 | 0.50 | 2.82 | 20.74 | 153 | −18.60 | 40.40 | ... |
| 1274 | ... | 14.37 | 0.57 | 6.91 | 20.58 | 99 | −20.61 | 41.65 | 21.89 |
| 1400 | ... | 16.45 | 0.17 | 4.49 | 20.57 | 176 | −19.78 | 41.24 | ... |
| 1438 | ... | 16.52 | 0.33 | 3.01 | 20.81 | 109 | −18.67 | 40.66 | ... |
| 1578 | ... | 15.85 | 0.40 | 3.11 | 20.12 | 114 | −19.43 | 41.64 | 21.71 |
| 1637 | ... | 16.30 | 0.33 | 4.46 | 20.89 | 141 | −19.44 | 41.14 | ... |
| 1664 | ... | 15.33 | 0.60 | 5.96 | 20.62 | 136 | −20.34 | 41.66 | 22.22 |
| 1870 | ... | 15.66 | 0.59 | 2.99 | 20.71 | 76 | −18.75 | 41.09 | ... |
| 2079 | ... | 16.80 | 0.52 | 3.17 | 20.84 | 129 | −18.75 | 41.20 | ... |

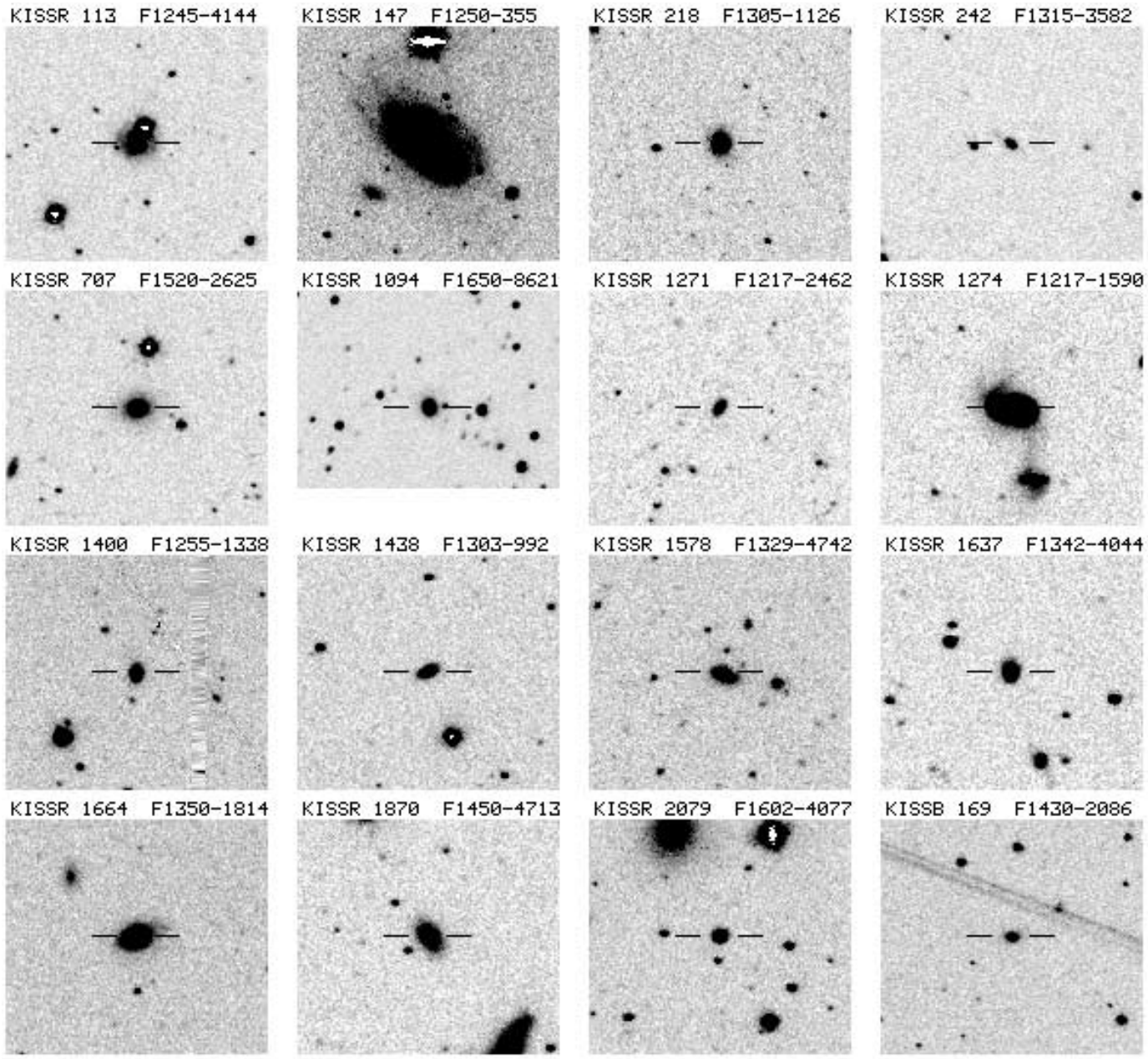


FIG. 6.—Images of all 16 LCBG candidates. These images are derived from the survey images and represent a composite of the *B* and *V* filter direct images. The LCBG candidates are located in the center of each image (*tick marks*). For the KR1 and KB1 galaxies (KISSR $< 1128$, plus KISSB 169) the images cover a field of view (FOV) of $4.'5 \times 4.'0$, while those from KR2 (KISSR $> 1128$) have FOVs of $3.'2 \times 2.'9$. North is up, and east is left in all images.

us to examine the properties of the KISS LCBG candidates in some detail. In this subsection, we present the properties of the LCBG candidates and a comparison sample of KISS SFGs with $M_B < -18.5$. When the necessary data are available, we also present the CS comparison sample of "normal" galaxies that have $M_B < -18.5$. All three of these samples are taken from the same volume of space (same area of the sky and $D < 185$ Mpc). One implication of this distance limit is that the galaxies in our KISS comparison sample have lower luminosities and bluer colors than the overall sample of star-forming KISS galaxies. In general, the most distant galaxies in any sample tend to be the most luminous, and galaxies that are more luminous tend to be redder.

The *B*-band absolute magnitudes of the KISS LCBGs, KISS SFGs, and CS magnitude-limited sample are plotted against $SB_e$ in Figure 7. Together with Figure 4, these two plots exhibit the selection criteria of the LCBG candidates and also illustrate nicely the properties of the three galaxy samples. As pointed out in § 2.3, the KISS SFG comparison sample exhibits a fairly continuous distribution in all three parameters, $SB_e$, $M_B$, and $B - V$ color, with the LCBG candidates representing the extreme cases in terms of color and surface brightness (Fig. 4). The CS and KISS SFG samples overlap substantially in both Figures 4 and 7, although the latter are on average much bluer. The LCBG candidates are seen to be distributed fairly evenly in absolute magnitude between $-18.6$ and $-20.6$. They define the upper envelope of the KISS ELGs in Figure 7.

Figure 8 shows histograms of the half-light diameters of the LCBG candidates, the KISS comparison sample SFGs, and the CS comparison sample "normal" galaxies. The median

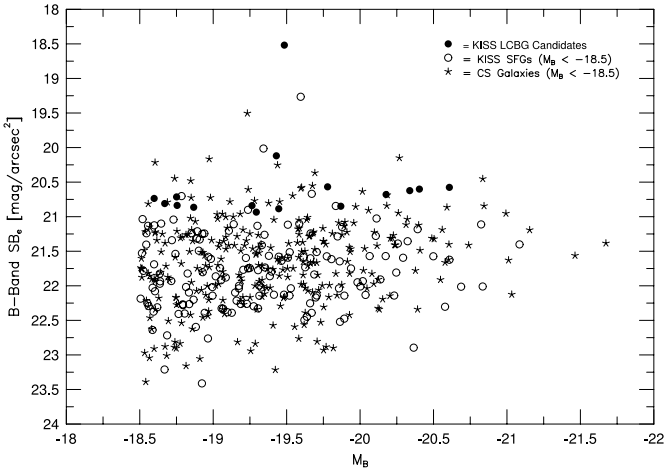


FIG. 7.—Projection of effective *B*-band surface brightness against absolute *B*-band magnitude for the KISS SFGs and CS galaxies within 185 Mpc of the Milky Way, showing galaxies from the CS (*stars*), the KISS SFGs (*open circles*), and the distance-limited LCBG sample (*filled circles*).

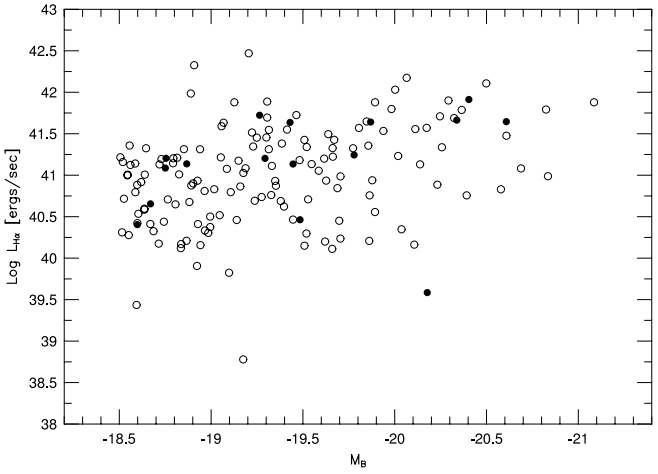


FIG. 9.—H$\alpha$ luminosities vs. absolute *B*-band magnitudes for the 16 KISS LCBG candidates (*filled circles*) and the comparison sample of KISS SFGs (*open circles*). The median $\log L_{H\alpha}$ of this LCBG sample is 41.21 ergs s$^{-1}$, which is approximately 1.6 times more luminous than the median $\log L_{H\alpha}$ of the comparison sample, 41.01 ergs s$^{-1}$.

diameters for the three samples, 4.11, 6.63, and 6.43 kpc, respectively, are indicated in the figure. As expected, the KISS LCBGs, on average, are 60% smaller than the CS galaxies and SFGs. The largest LCBGs have sizes comparable to the medians for the other two distributions. Since the samples have comparable luminosities, the difference in diameter accounts for most of the difference in $SB_e$.

Figure 9 shows the H$\alpha$ luminosity plotted against $M_B$ for the two KISS samples. The sample of 16 KISS LCBG candidates exhibits a higher median H$\alpha$ luminosity by a factor of 1.6 than the comparison sample SFGs. Because we consider only active SFGs in both samples, we can draw an important conclusion from this result. In general, the H$\alpha$ luminosity indicates the activity level of a galaxy, telling us how many ionizing stars a galaxy contains. The KISS LCBG candidates have, on average, 60% higher current star formation rates than the less compact SFGs. There is a clear tendency for the LCBG candidates to be located near the top of the diagram, again illustrating that they are above average relative to the comparison sample. Note that not all the LCBG candidates are in the high star formation rate category. One of the KISS ELGs with the *lowest* H$\alpha$ luminosity, KISSR 147, happens to be included among the LCBGs. We note in passing that the measurement of the H$\alpha$ flux in this object may well be underestimated, since it is so extended on the sky and since the star formation appears to be spread over a large fraction of the galaxy. The KISS objective-prism flux measurement is made over an 8″ wide region centered on the galaxy. Hence, our current estimate for the H$\alpha$ luminosity of KISSR 147 may be significantly lower than the actual value. We do not believe that this problem occurs for any of the other KISS LCBGs.

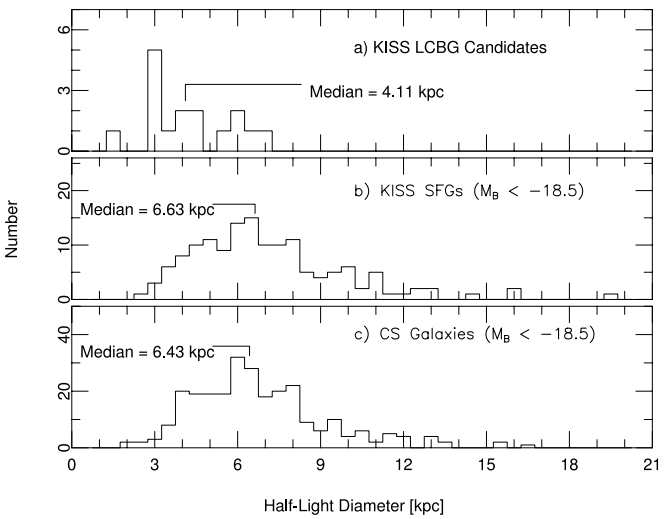


FIG. 8.—Distribution of the derived diameters in kiloparsecs for the 16 KISS LCBG candidates, the comparison sample of KISS SFGs, and the comparison sample of CS galaxies. The median diameter of the LCBG sample is 4.11 kpc, the median diameter of the KISS comparison sample is 6.63 kpc, and the median diameter of the CS comparison sample is 6.43 kpc.

It is also relevant to consider the spectral properties of the LCBG candidates. Do their spectra reveal any systematic differences relative to the less compact SFGs of the KISS sample? We try to explore this question in two ways. First, in Figure 10 we plot an emission-line ratio diagnostic diagram showing the locations of all the KISS SFGs (regardless of distance). We plot the logarithms of the [O III]/H$\beta$ ratio versus the [N II]/H$\alpha$ ratio. The open circles show the "regular" SFGs, while the filled circles indicate the location of the 15 LCBG candidates with measured line ratios. The diagram reveals the characteristic H II sequence, where the SFGs fall along an arc in the diagram stretching from the top left (typically lower luminosity, lower metallicity galaxies) to the bottom right (typically more luminous, higher metallicity objects). The LCBGs are distributed fairly uniformly along the lower two-thirds of the arc. Our selection against lower luminosity galaxies prevents them from falling in the top left portion of the H II sequence. We detect no obvious trends among the LCBGs that would lead us to believe that their spectral properties are systematically different from the rest of the KISS SFGs.

We also consider the metal abundances [$\log(O/H) + 12$] of these 15 LCBG candidates compared with the sample of all KISS SFGs within 185 Mpc of the Milky Way. Using the linear luminosity-metallicity (*L*-*Z*) relation of Melbourne & Salzer (2002), we plot metal abundance versus absolute magnitude for the KISS SFGs. Figure 11 shows a weak tendency for the LCBGs, shown as filled circles on the plot, to lie at or below the mean *L*-*Z* relation. The mean abundance of the

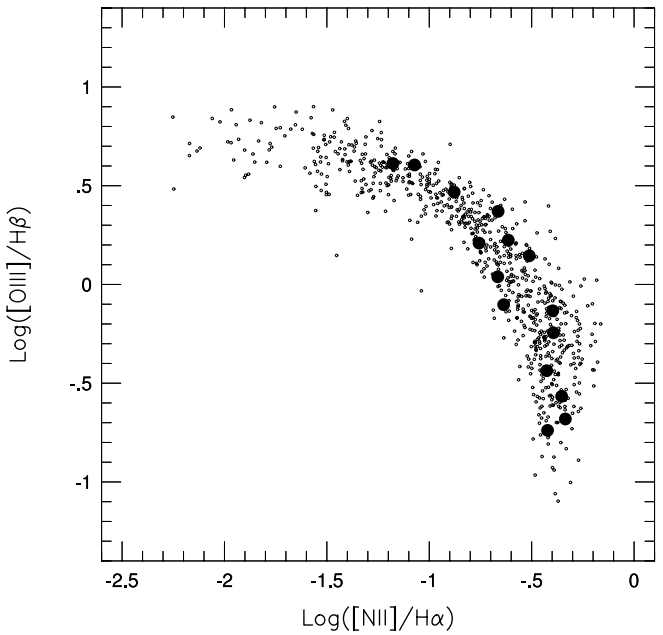


FIG. 10.—Logarithm of [O III]/H$\beta$ vs. the logarithm of [N II]/H$\alpha$ for all KISS SFGs. The large circles show the LCBG candidates. The characteristic H II sequence is shown by the KISS SFGs: the low luminosity, metal-poor galaxies fall in the top left of the diagram, and the high luminosity, metal-rich galaxies fall in the bottom right region. The KISS LCBGs do not appear to deviate from this sequence.

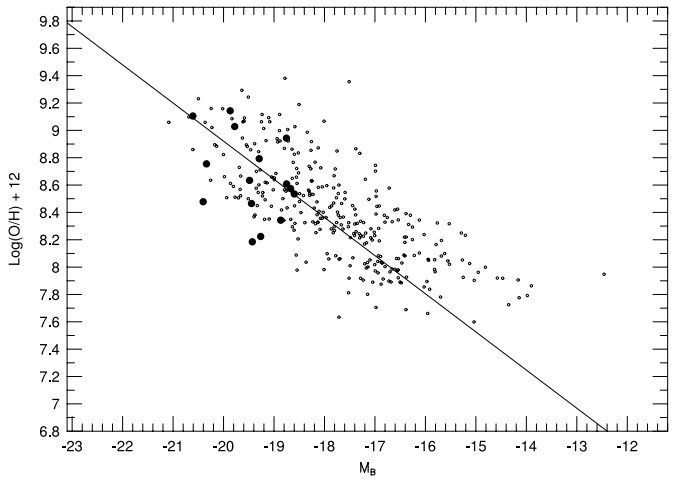


FIG. 11.—$M_B$ vs. the metal abundance [ $\log(\mathrm{O}/\mathrm{H}) + 12$] for KISS SFGs within 185 Mpc of the Milky Way, showing the 15 LCBG candidates with derived abundances (*filled circles*) on this plot, the KISS SFGs (*open circles*), and the linear *L-Z* fit for KISS galaxies derived in Melbourne & Salzer (2002; *line*).

15 LCBGs is 8.65, compared with the mean abundance of the comparison sample (KISS SFGs with $D < 185$ Mpc and $M_B < -18.5$) of 8.75. The statistical significance of this 0.1 dex difference is minimal, since the formal error in the difference of the two means is 0.08. Still, this small difference may suggest that either the LCBGs are underproducing heavy elements compared with the comparison SFGs, the LCBGs are systematically losing a larger fraction of their metals via outflows, or the enhanced star formation of the LCBGs is producing a modest luminosity enhancement relative to the rest of the SFGs. While it is not possible to definitively select between these options, the high current star formation rates exhibited by the LCBGs would appear to be inconsistent with the first of these choices, while the higher central mass densities implied by the high $\mathrm{SB}_e$ of the LCBGs is inconsistent with the second (see discussion in Salzer et al. 2004). Hence, we conclude that the LCBG candidates appear to be offset slightly to the left of the KISS SFGs, indicating that their luminosities may not be representative of their masses. While this latter point is likely true in general, for all SFGs (e.g., Lee et al. 2004), it appears to be even more the case for the LCBG sample.

### 3.2. *Radio Continuum Emission*

To some extent, all galaxies exhibit radio emission, but those that are the most radio-luminous are known historically as "radio galaxies." Because SFGs are often radio sources, we investigate the radio properties of the LCBG candidates compared with a sample of all KISS SFGs and expect to detect radio emission for some subset of our samples. All radio fluxes cited in this work come from Van Duyne et al. (2004), who used the FIRST (Becker et al. 1995) and NRAO VLA Sky Survey (NVSS; Condon et al. 1998) 20 cm radio continuum surveys to study the radio emission associated with the 2158 KISS ELGs from KR1 and KR2. Because that study did not include the KB1 portion of KISS, we exclude the KB1 ELGs from this part of our analysis.

Of all KISS ELGs known to be SFGs in the KR1 and KR2 survey strips, 13.7% are detected by FIRST and NVSS in the radio. This is an upper limit to the fraction of radio detections, however, since only 57.6% of the KR1 and KR2 galaxies currently have follow-up spectra (note that *all* the radio-detected KISS galaxies possess follow-up spectra). If we assume that $\sim$90% of the galaxies lacking follow-up spectra are also SFGs, then the fraction of SFGs with radio continuum detections drops to only 7.4%. This latter value is likely to be closer to the actual percentage of radio-detected SFGs. We compare this number with the fraction of radio galaxies within our LCBG candidate sample (from only KR1 and KR2) and with the fraction of radio galaxies within our distance-limited comparison sample of KR1 and KR2 SFGs with $M_B < -18.5$. Fully 53% of the 15 LCBG candidates have detectable radio continuum emission, while 28% of the comparison sample galaxies have detected radio fluxes.

The LCBGs clearly have a stronger propensity to possess detectable radio emission. We hypothesize that the intense star-forming activity indicated by the high $\mathrm{SB}_e$ of the LCBG candidates is the primary contributor to this effect. In SFGs, the energy given to the relativistic electrons, which cause synchrotron radiation, comes from the supernova explosions occurring over the past $\sim 3 \times 10^7$ yr (Cram 1998). Presumably, the KISS LCBGs produce more supernovae in this period than regular SFGs because of their above-average SFRs (§ 3.1). In addition, because of their compact nature, LCBGs may have stronger magnetic fields than normal SFGs. These properties, in concert, enhance the detectability of synchrotron radiation in LCBGs relative to other SFGs.

Despite the high proportion of radio detections among the LCBGs, their radio powers do not stand out. For the eight detected LCBGs, the mean radio power is $10^{21.81}$ W Hz$^{-1}$. This is statistically indistinguishable from the mean of the distance-limited comparison sample ($10^{21.84}$ W Hz$^{-1}$) and significantly less than the average of all KISS SFGs detected by FIRST and NVSS ($10^{22.11}$ W Hz$^{-1}$). The majority of the overall radio-detected SFGs lie at distances beyond 185 Mpc, so it is no surprise that their radio luminosities are higher. However, it is

perhaps a bit surprising that the LCBGs do not have higher radio powers than the comparison SFGs. Of course, the number of LCBGs in this analysis is small, so it may be premature to draw strong inferences regarding the radio powers at this time. What is clear, however, is that the LCBGs are more commonly detected as radio emitters than are the overall population of SFGs in the same volume.

### 3.3. *Volume Density of Local LCBGs*

The space density of the intermediate- and high-redshift LCBGs compared with that of low-redshift LCBGs acts as an essential constraint on their density evolution. Nearly all previous studies of LCBGs stress their apparent extreme density evolution. For our sample of LCBG candidates with $z < 0.045$, we compute the volume density using the $1/V_{\max}$ method. A complete description of this method, along with the specific completeness parameters used in the calculations, can be found in C. Gronwall et al. (2004, in preparation). In brief, we first determine whether the detectable volume of an individual galaxy is limited by the effective volume set by the KISS redshift limit or by its own emission-line flux. Then, for all galaxies in this sample, we sum the inverse of the maximum volume within which each galaxy is detectable. Accordingly, we determine the space density of local LCBGs to be $5.4 \times 10^{-4}\ h_{75}^3$ Mpc$^{-3}$. To arrive at an estimate of the uncertainty in the volume density, we assume that the main source of error is the Poissonian uncertainty in the number of LCBGs (i.e., $\sigma = \sqrt{N}$). This is reasonable, since the uncertainties in the line flux completeness limits and the relevant volumes are fairly small. Hence, since there are 16 LCBGs in the distance-limited sample, the computed volume density carries with it a 25% uncertainty.

A handful of previous studies have derived estimates for the space densities of LCBGs at intermediate and high redshifts. For example, Phillips et al. (1997) find the volume density of LCBGs at redshifts between 0.4 and 0.7 with $M_B < -18.5$ to be $2.2 \times 10^{-3}\ h_{75}^3$ Mpc$^{-3}$ and that of LCBGs at redshifts between 0.7 and 1.0 with $M_B < -18.5$ to be $8.8 \times 10^{-3}\ h_{75}^3$ Mpc$^{-3}$. Lowenthal et al. (1997) estimate a total space density of the high-redshift ($2.2 < z < 3.5$) population of LCBGs to be $3.7 \times 10^{-3}\ h_{75}^3$ Mpc$^{-3}$. This latter density estimate must be taken as a lower limit, since the objects in the Lowenthal et al. sample are at such high redshifts that only the most luminous sources are detectable. A correction to account for the incompleteness at the lower luminosities would likely raise the density estimate substantially. A large (and probably rather uncertain) incompleteness correction to account for missing lower luminosity LCBGs was applied by Phillips et al. to their higher redshift subsample. Because of the large uncertainties associated with the LCBG density estimates in these higher redshift samples, one should use caution in interpreting the numbers. We estimate that the uncertainties in these densities, including any errors associated with the incompleteness corrections, must be at least 33% for the lower redshift value of Phillips et al. and closer to 50% for the two higher redshift estimates.

The uncertainty that arises from different absolute magnitude cutoffs at different redshifts can be alleviated somewhat by applying a *brighter* cutoff to our sample. By making our local sample's luminosity limit consistent with the absolute magnitude limit of the higher $z$ samples, rather than extrapolating the high-$z$ absolute magnitudes to lower luminosities (as was done by Phillips et al. [1997], as described above), one avoids introducing some large and very uncertain corrections. For example, Phillips et al. (1997) had an absolute magnitude limit of $-20$ (using $H_0 = 50$ km s$^{-1}$ Mpc$^{-1}$) for their sample at $0.7 < z < 1.0$, which corresponds to an absolute magnitude limit of $-19.12$ for $H_0 = 75$ km s$^{-1}$ Mpc$^{-1}$. We derive a volume density of $3.9 \times 10^{-4}\ h_{75}^3$ Mpc$^{-3}$ for our sample of local LCBGs when we adopt $M_B < -19.12$ as our luminosity limit. For comparison, Phillips et al. (1997) find the volume density of LCBGs at redshifts between 0.7 and 1.0 with $M_B < -19.12$ to be $4.05 \times 10^{-3}\ h_{75}^3$ Mpc$^{-3}$. We note that this method is impractical to use for the Lowenthal et al. sample (1997) and unnecessary when comparing with the lower redshift Phillips et al. sample.

With the above caveats in mind, we compare the volume densities of LCBGs from our local ($z = 0$) sample with those of the higher redshift studies. The value Phillips et al. (1997) obtain for their lower redshift sample implies that the volume density of LCBGs has declined by a factor of $\sim$4 between $z \sim 0.5$ and the present, while their higher redshift value suggests that the density of LCBGs has dropped by a factor of $\sim$16 between $z \sim 0.85$ and today. This latter factor becomes $\sim$10 for the comparison using the volume density of the KISS LCBGs with $M_B < -19.12$. The density drop implied by Lowenthal et al. (1997) for the high-redshift LCBGs ($2.2 < z < 3.5$) is at least a factor of $\sim$7 and is likely to be much higher. The work of Lilly et al. (1996, 1998), Phillips et al. (1997), and Mallén-Ornelas et al. (1999) all suggest that the volume density of LCBGs drops off by a factor of $\sim$10 from $z = 1$ to the present. This prediction is in general agreement with the results presented here, given the large errors associated with the density estimates; that is, the space density derived for our sample of LCBGs compared with that of the higher redshift samples supports the claim that these galaxies are indeed a strongly evolving population. However, the uncertainties associated with the volume density of LCBGs at higher redshifts precludes an accurate assessment of exactly how extreme their evolution is. We hope that future studies of high-redshift LCBG populations will constrain their volume densities more definitively and lead to a better understanding of their evolution with look-back time.

## 4. DISCUSSION

This paper deals with the problem of LCBGs by approaching only one of its facets; namely, we have sought to identify local examples of LCBGs in an effort to constrain the properties of those LCBGs present in such profusion at intermediate and high $z$. However, we must be cautious in accepting that our sample is composed of genuine LCBGs—indeed, we call the galaxies in our sample "LCBG candidates." The classification scheme for LCBGs presented by Jangren et al. (2004, in preparation) defines a six-dimensional parameter space in which LCBGs are effectively isolated from other types of galaxies. However, we could not apply this method for our LCBG selection, as KISS direct images did not have the resolution required to perform the prescribed tests. Furthermore, while Jangren et al. conclude that the parameter space of $B - V$ color versus $SB_e$ is the best for separating the LCBGs from other types of galaxies, they acknowledge that there is still no single cut that will eliminate all non-LCBGs nor include all bona fide LCBGs.

Specifically, employing a color limit to select local LCBGs on the basis of the corrected rest-frame colors of higher redshift LCBGs is a bit problematic. The many corrections that must be applied to color (i.e., $K$-corrections, Galactic reddening, internal extinction, and emission-line contamination) make it a difficult parameter to use to define a sample of galaxies. In addition, the rest-frame colors of SFGs at high redshift are

inherently biased to be bluer than those of lower redshift SFGs. This is because host galaxies at higher redshift have not had as much time to assemble as those in the nearby universe. Hence, they are intrinsically less luminous, and a star formation event at high $z$ tends to dominate the galactic color more than at lower redshifts. Accounting for this effect, however, would be a difficult task, mainly because of the uncertainty in our understanding of galaxy evolution.

The necessity of a color parameter, however, is manifest in Figure 4. Luminous elliptical galaxies from the CS meet both the luminosity and surface brightness criteria for LCBGs. However, LCBGs are not similar to local elliptical galaxies. A color cut acts as the means for excluding early-type galaxies in traditional, magnitude-limited surveys. By contrast, in ELG surveys such as KISS that contain few, if any, elliptical galaxies, the color criterion becomes less pertinent. Limiting the samples of LCBGs to active SFGs should ensure their relative blueness. While not extremely blue compared with other SFGs, the KISS LCBG candidates are considerably bluer than "normal" galaxies. The CS "normal" field galaxies within the distance limit of 185 Mpc have a median $B - V$ color of 0.77, considerably higher than the median color of the LCBG sample, 0.44. Had we selected a sample of LCBGs using only the luminosity and surface brightness criteria and limiting our sample to only active SFGs, our sample would have contained 22 KISS LCBG candidates with a median $B - V$ color of 0.53, still considerably bluer than the CS galaxies.

We select our local samples of LCBGs only from active SFGs not only as a way to ensure their relative blueness, but also to further constrain their properties to match those of the higher redshift samples. Indeed, all known LCBGs at high $z$ are vigorously forming stars, as evidenced by their strong emission lines. This property gives rise to important questions regarding the nature of LCBGs. Is active star formation always present in galaxies meeting the LCBG selection criteria? Can an LCBG be an LCBG without its starburst? What do LCBGs look like when and if the star formation fades? Do the LCBG criteria allow for nonactive galaxies?

In an attempt to address these questions, we looked at the galaxies located in the KISS database that are *not* ELGs but rather galaxies detected by the CS that have measured redshifts, colors, and absolute magnitudes. Since the first two survey lists of KISS (KR1 and KB1) overlap parts of the CS, we possess direct images taken through $B$ and $V$ filters of essentially all the CS galaxies. By combining our imaging photometry with the CS redshifts (Wegner et al. 2001), we are able to carry out the same analysis on the CS galaxies as we previously did for the KISS ELGs. Applying the same cutoffs in $SB_e$, $M_B$, and $B - V$ color to these galaxies yields a sample of seven CS LCBG candidates. Of these, only three were not also detected by KISS. All three lie outside the area of sky covered by KR1. One of these galaxies has been identified using the NASA Extragalactic Database[2] as a nearby Seyfert 2 galaxy with very weak emission lines. KISS could not have detected this galaxy because of its strong continuum and the weakness of its H$\alpha$ line. The others were initially detected by the Case Low-Dispersion Northern Sky Survey (Sanduleak & Pesch 1984), with published follow-up spectroscopy in Salzer et al. (1995). One galaxy, CG 60, is an SFG with strong H$\alpha$ and weak O III. The other, CG 90, appears to be a weak-lined SFG, possibly a poststarburst system. This latter galaxy appears to be the closest thing to a "normal" (i.e., not actively star forming) galaxy in the $\sim$100 deg$^2$ of the CS that meets the LCBG selection criteria. However, even CG 90 has *some* current star formation. The study by Drinkwater et al. (1999), which used the Fornax Spectroscopic Survey to find a sample of bright compact galaxies that are unresolved on photographic plates, obtains a similar result. Of their 13 local ($z < 0.21$) galaxies that resemble the higher $z$ LCBGs, they find only four that do not have strong emission lines. One of the galaxies has a poststarburst spectrum, and another has a spectrum indicating an old population.

This paucity of nonactive LCBGs suggests that, in general, they are extremely rare and that perhaps the star formation that always seems to be present in LCBGs is a key factor in labeling them as LCBGs in the first place. Clearly, the star formation activity helps to make the LCBG. The starburst both increases the central luminosity of the galaxy and shortens the half-light radius $r_{\rm hl}$. These two effects combine to increase $SB_e$ and lower the color. Is a central starburst *required* for a galaxy to become an LCBG? Perhaps not, but it certainly appears to be strongly favored.

While it is possibly premature to attempt to resolve the questions regarding the evolution of LCBGs discussed in § 1, we can at least use the properties of the local candidates to speculate a bit. The distribution of the KISS ELGs in Figure 4 suggests that they exhibit a continuum of physical characteristics in the surface brightness, color, and luminosity parameter space. Galaxies classified as LCBGs using the Jangren et al. selection criteria represent those galaxies that currently lie at the extreme end of that continuum. Clearly, however, there are plenty of KISS ELGs that are located just below the surface brightness threshold that distinguishes our LCBG candidates from the remainder of the SFG population. Since the KISS LCBGs do, on average, exhibit higher H$\alpha$ luminosities, it is likely that at least some of them evolve out of the LCBG region in Figure 4 as their starbursts fade. Will they fade substantially, as proposed by Koo et al. (1995) and Guzmán et al. (1998), dropping in luminosity by 4 mag or more, becoming substantially redder and more gas-poor and eventually resembling dwarf elliptical galaxies?

We feel that it is unlikely that any of our LCBG candidates will evolve into early-type galaxies. The evolutionary scenario proposed by Koo et al. (1995) and Guzmán et al. (1998) requires that the gas present in the LCBG be removed, presumably by strong supernovae-driven outflows. Hydrodynamic models (e.g., Mac Low & Ferrara 1999) suggest that this complete blow-away of a galaxy's intergalactic medium does not occur for any but the least massive systems. Therefore, we do not expect any of our current sample of LCBGs to become gas-poor and fade into red ellipticals. Of course, it remains possible that the higher redshift LCBGs represent a more heterogeneous sample of objects (Guzmán et al. 1997; Phillips et al. 1997; Hammer et al. 2001; Pisano et al. 2001; Garland et al. 2004). If some of the high-$z$ LCBGs had lost their gas and evolved into dwarf elliptical galaxies by the present time, our selection method would not be sensitive to them. However, based on the models of Mac Low & Ferrara, we would expect that the majority of LCGBs should retain their gas to the current epoch. This appears to be the case with our sample.

The continuum of physical characteristics evident in Figure 4 suggests that luminous galaxies possess a range in the ratio of their central surface brightnesses to central mass densities. This has been observed in dwarf galaxies (e.g., Papaderos et al.

[2] This research has made use of the NASA/IPAC Extragalactic Database, which is operated by the Jet Propulsion Laboratory, California Institute of Technology, under contract with the National Aeronautics and Space Administration.

1996; Salzer & Norton 1999), in which the most actively star-forming dwarf galaxies (aka blue compact dwarfs [BCDs]) are seen to lie at the extreme end of a continuum that stretches to very low central surface brightnesses at the other extreme. Furthermore, the gas distributions in the BCDs are seen to be much more centrally concentrated than those in more quiescent dwarf irregular galaxies (e.g., van Zee et al. 1998). The combination of high central mass densities and high central gas densities makes BCDs particularly efficient at forming stars. We assume that this is no accident: BCDs are by their nature well equipped to be making stars. By analogy, one might argue that LCBGs are predisposed to make stars efficiently because they too represent the extreme high surface brightness, high central mass density end of a continuous distribution, albeit for more luminous galaxies. In this picture, LCBGs are preferentially in a star-forming phase for a large fraction of the time. When not undergoing a strong starburst, they fade somewhat (mostly in $SB_e$ but also slightly in color and luminosity) and join the population of galaxies lying below the LCBG selection region in Figure 4. This would help explain the lack of *any* non–star-forming LCBGs present among the CS galaxies. Even when not strongly bursting, post-LCBGs may exhibit a modest level of star formation, such as that seen in CG 90. The question of where the large population of LCBGs seen at $z = 0.5$–$1.0$ has gone is then resolved, at least in part, by the population of less active SFGs seen in Figure 4. The large number of KISS ELGs located below the LCBG selection region in this plot appears to account for a large fraction of the "missing" LCBGs. The drop in density of LCBGs may be directly linked to the fall in the star formation rate density between $z = 1$ and the present (e.g., Madau et al. 1996, 1998). The galaxies still exist; they are simply in a somewhat less active state. In this scenario, LCBGs are not pathological outliers but rather the most compact galaxies at the extreme end of a continuous distribution of gas-rich SFGs.

It should be relatively simple to test the above hypothesis. A combination of high spatial resolution surface photometry in the optical and Very Large Array (VLA) H I mapping in the radio could be used to evaluate the stellar and gas mass distributions of the local LCBG candidates. A direct comparison of these properties between the LCBGs and a sample of "normal" galaxies would reveal whether our LCBGs are structurally different from the non-LCBGs. These same observations would be extremely helpful in establishing their dynamical masses as well. This latter parameter is essential for showing clearer linkage between the local samples of LCBGs with the intermediate- and high-redshift analogs. Efforts are already underway in this regard. As a first step in determining gas and dynamical masses, we have obtained single-dish H I observations with the Arecibo 305 m radio telescope for the sample of LCBGs accessible from Arecibo, along with a control sample of "normal" SFGs. With these data, we will derive H I masses and provide at least a rough estimate for the dynamical masses (J. K. Werk et al. 2004, in preparation) for our LCBGs. We will also be able to ascertain which of our galaxies would be suitable for follow-up VLA mapping. In addition, we have begun acquiring higher resolution optical images of our LCBGs, with the goal of being able to perform detailed surface photometry. In addition, these more detailed images will allow us to carry out a morphological analysis of our sample of local LCBGs that will provide clues as to whether their intense starbursts are caused by mergers and/or interactions or are simply the result of their intrinsically compact nature. Finally, emission-line widths measured from high-resolution spectra combined with near-infrared images and our H I mass estimates could settle the debate about the masses of LCBGs.

## 5. SUMMARY AND CONCLUSIONS

In this paper, we present a sample of local analogs to the intermediate- and high-$z$ LCBGs. We selected our sample from only those KISS galaxies that are actively forming stars. Because of resolution effects, we limit our sample to only those galaxies within 185 Mpc of the Milky Way. The sample of LCBGs is defined by the following criteria: a surface brightness limit of $SB_e < 21.0$ mag arcsec$^{-2}$, an absolute magnitude limit of $M_B < -18.5$, and a color cutoff of $B - V < 0.6$ with $H_0 = 75$ km s$^{-1}$ Mpc$^{-1}$. A total of 16 KISS SFGs meet these criteria.

We have compared some of the properties of the KISS LCBG candidates with those of a comparison sample of KISS SFGs and a comparison sample of CS galaxies that are supposed to represent "normal galaxies." On average, the KISS LCBG candidates have a higher tendency to emit detectable radio continuum flux; have higher H$\alpha$ luminosities, indicating strong star formation properties; have slightly lower than expected metal abundances for KISS galaxies of their luminosity; and have considerably smaller sizes than those galaxies in both the KISS and CS comparison samples. We have calculated the volume density for the sample of local LCBG candidates to be $5.4 \times 10^{-4}\ h_{75}^3$ Mpc$^{-3}$. This value indicates a substantial density evolution of LCBGs, which is in general agreement with the predictions made by Lilly et al. (1996, 1998), Phillips et al. (1997), and Mallén-Ornelas et al. (1999). However, precise estimates of the density evolution of the LCBGs are difficult, because of the large uncertainties in the values of the volume density for higher redshift populations. We have utilized the CS database in an attempt to select a sample of local nonactive LCBGs to constrain the density of non–star-forming LCBGs. We found no additional non–star-forming LCBGs, although one weakly star-forming (possibly poststarburst) galaxy was recognized. We postulate that LCBGs are structurally predisposed for star formation and that their compact nature may indicate a high central gas concentration that drives ongoing star formation.

The need for a local sample of LCBGs is well documented. Much of the published work on these galaxies speaks to the need for a representative local comparison sample that will help settle the debates over their size, mass, morphology, and low-redshift counterparts. We conclude that our sample of local LCBG candidates contains galaxies that are likely to be local versions of the more distant LCBGs. This local sample provides the starting point in our ongoing study of the properties and evolution of LCBGs.

Funding for this work was provided by an NSF Presidential Faculty Award to J. J. S. (NSF AST 95-53020). Additional support for our ongoing follow-up spectroscopy campaign came from continued funding from the NSF (AST 00-71114) and Wesleyan University. We are grateful to the anonymous referee for several helpful suggestions that improved the presentation. We thank the numerous KISS team members who have participated in spectroscopic follow-up observations during the past several years, particularly Caryl Gronwall, Drew Phillips, Gary Wegner, Jason Melbourne, Laura Chomiuk,

Kerrie McKinstry, Robin Ciardullo, and Vicki Sarajedini. Special thanks to Rafael Guzmán for providing us with information about selection criteria for LCBGs and for several useful discussions. Finally, we wish to thank the support staffs of Kitt Peak National Observatory, Lick Observatory, the Hobby-Eberly Telescope, MDM Observatory, and Apache Point Observatory for their excellent assistance in obtaining the survey data, as well as the spectroscopic observations.

REFERENCES

Barton, E. J., & van Zee, L. 2001, ApJ, 550, L35
Becker, R. H., White, R. L., & Helfand, D. J. 1995, ApJ, 450, 559
Condon, J. J., Cotton, W. D., Griesen, E. W., Yin, Q. F., Perley, R. A., Taylor, G. B., & Broderick, J. J. 1998, AJ, 115, 1693
Cram, L. E. 1998, ApJ, 506, L85
Drinkwater, M. J., Phillips, S., Gregg, M. D., Parker, Q. A., Smith, R. M., Davies, J. I., Jones, J. B., & Sadler, E. M. 1999, ApJ, 511, L97
Frei, Z., Guhathakurta, P., Gunn, J. E., & Tyson, J. A. 1996, AJ, 111, 174
Garland, C. A., Pisano, D. J., Williams, J. P., Guzmán, R., & Castander, F. J. 2004, ApJ, 615, 689
Geller, M. J., et al. 1997, AJ, 114, 2205
Gronwall, C., Jangren A., Salzer, J. J., Werk, J. K., & Ciardullo, R. 2004a, AJ, 128, 644
Gronwall, C., Salzer, J. J., Sarajedini, V. L., Jangren, A., Chomiuk, L., Moody, J. W., Frattare, L. M., & Boroson, T. A. 2004b, AJ, 127, 1943 (KR2)
Guzmán, R. 2001, Ap&SS, 277, 507
———. 2003, in Proc. ESO/USM/MPE Workshop on Multiwavelength Mapping of Galaxy Formation and Evolution, ed. R. Bender & A. Renzini (Berlin: Springer)
Guzmán, R., Gallego, J., Koo, D. C., Phillips, A. C., Lowenthal, J. D., Faber, S. M., Illingworth, G. D., & Vogt, N. P. 1997, ApJ, 489, 559
Guzmán, R., Jangren, A., Koo, D. C., Bershady, M. A., & Simard, L. 1998, ApJ, 495, L13
Guzmán, R., Koo, D. C., Faber, M., Illingworth, G., Takamiya, M., Kron, R. G., & Bershady, M. A. 1996, ApJ, 460, L5
Guzmán, R., Östlin, G., Kunth, D., Bershady, M. A., Koo, D. C., & Pahre, M. A. 2003, ApJ, 586, L45
Hammer, F., Gruel, N., Thuan, T. X., Flores, H., & Infante, L. 2001, ApJ, 550, 570
Koo, D. C., Bershady, M. A., Wirth, G. D., Stanford, S. A., & Majewski, S. R. 1994, ApJ, 427, L9
Koo, D. C., Guzmán, R., Faber, S. M., Illingworth, G. D., Bershady, M. A., Kron, R. G., & Takamiya, M. 1995, ApJ, 440, L49
Koo, D. C., & Kron, R. G. 1992, ARA&A, 30, 613
Lee, J. C., Salzer, J. J., & Melbourne, J. 2004, ApJ, 616, 752
Lilly, S., Le Févre, O., Hammer, F., & Crampton, D. 1996, ApJ, 460, L1
Lilly, S. J., et al. 1998, ApJ, 500, 75
Lowenthal, J. D., et al. 1997, ApJ, 481, 673
Mac Low, M., & Ferrara, A. 1999, ApJ, 513, 142
Madau, P., Ferguson, H. C., Dickinson, M. E., Giavalisco, M., Steidel, C. C., & Fruchter, A. 1996, MNRAS, 283, 1388
Madau, P., Pozzetti, L., & Dickinson, M. E. 1998, ApJ, 498, 106
Mallén-Ornelas, G., Lilly, S. J., Crampton, D., & Schade, D. 1999, ApJ, 518, L83
Melbourne, J., Phillips, A. C., Salzer, J. J., Gronwall, C., & Sarajedini, V. L. 2004, AJ, 127, 686
Melbourne, J., & Salzer, J. J. 2002, AJ, 123, 2302
Östlin, G., Amram, P., Bergvall, N., Masegosa, J., Boulesteix, J., & Márquez, I. 2001a, A&A, 374, 800
Östlin, G., Amram, P., Boulesteix, J., Bergvall, N., Masegosa, J., & Márquez, I. 2001b, Ap&SS, 277, 433
Papaderos, P., Loose, H. H., Fricke, K. J., & Thuan, T. X. 1996, A&A, 314, 59
Phillips, A. C., Guzmán, R., Gallego, J., Koo, D. C., Lowenthal, J. D., Vogt, N. P., Faber, S. M., & Illingworth, G. D. 1997, ApJ, 489, 543
Pisano, D. J., Kobulnicky, H. A., Guzmán, R., Gallego, J., & Bershady, M. A. 2001, AJ, 122, 1194
Salzer, J. J., Lee, J. C., Melbourne, J., Hinz, J., Alonso-Herrero, A., & Jangren, A. 2004, ApJ, submitted
Salzer, J. J., Moody, J. W., Rosenberg, J., Gregory, S. A., & Newberry, M. V. 1995, AJ, 109, 2376
Salzer, J. J., & Norton, S. A. 1999, in ASP Conf. Ser. 170, The Low Surface Brightness Universe, ed. J. I. Davies, C. Impey, & S. Phillipps (San Francisco: ASP), 253
Salzer, J. J., et al. 2000, AJ, 120, 80
———. 2001, AJ, 121, 66 (KR1)
———. 2002, AJ, 123, 1292 (KB1)
Sanduleak, N., & Pesch, P. 1984, ApJS, 55, 517
Schade, D., Lilly, S. J., Crampton, D., Hammer, F., Le Févre, O., & Tresse, L. 1995, ApJ, 451, L1
Schade, D., Lilly, S. J., Le Févre, O., Hammer, F., & Crampton, D. 1996, ApJ, 464, 79
Schlegel, D. J., Finkbeiner, D. P., & Davis, M. 1998, ApJ, 500, 525
Smail, I., Ivison, R. J., Blain, A. W., & Kneib, J. P. 1998, ApJ, 507, L21
Van Duyne, J., Beckerman, E., Salzer, J. J., Gronwall, C., Thuan, T. X., Condon, J. J., & Frattare, L. M. 2004, AJ, 127, 1959
van Zee, L., Skillman, E. D., & Salzer, J. J. 1998, AJ, 116, 1186
Wegner, G., Salzer, J. J., Gronwall, C., Jangren, A., & Melbourne, J. 2003, AJ, 125, 2373
Wegner, G., et al. 2001, AJ, 122, 2893